

Classification of Brain Tumours in MRI Images using VGG 19 Algorithm

Rahul Namdeo Jadhav^{*1,2}, G.Sudhagar¹

¹Department of ECE, Bharath Institute of Higher Education and Research, Tamilnadu, India

²AISSMS Institute of Information Technology, Pune, India

jadhavn@gmail.com, sudhagar.ece@bharathuniv.ac.in

ARTICLE INFO

ABSTRACT

Received: 29 Nov 2024

Revised: 14 Jan 2025

Accepted: 28 Jan 2025

For early identification and efficient treatment planning, brain tumour categorization is crucial. Deep learning in medical image analysis, models have lately shown remarkable outcomes, especially regarding MRI scan tumour categorization. This study proposes VGG-19 as the primary model and evaluates its performance against ResNet-50 and Google Net by comparing F1-score, AUC, precision, recall, and accuracy. Consequently, the suggested VGG-19 model had a maximum classification accuracy of 97.2%, outperforming GoogleNet at 96.4% and ResNet-50 at 95.3%. It proves from the confusion matrix that the classification of all kinds of tumours is superior, and minimal misclassifications are available with VGG-19. It is proven further by the ROC curve since AUC scored 0.97, giving excellent discrimination capability. GoogleNet was found to be competitive, especially in Glioma detection, while ResNet-50 provided a balanced classification in all classes. This outcome suggests that deep learning models, particularly VGG-19, efficiently classify brain tumour. Further studies can investigate transformer-based architectures, hybrid deep learning techniques, and the expansion of datasets to further enhance model generalization. Integration of explainable AI into medical imaging systems further improves transparency and clinical trust in using AI-assisted diagnosis in healthcare.

Keywords: Brain Tumor Classification, Deep Learning, VGG-19, MRI Imaging, Confusion Matrix, ResNet-50, GoogleNet.

INTRODUCTION

One of the most common illnesses in India is brain tumours. Many factors contribute to its spread, but a person's lifestyle is the most common. Brain tumours, which may be either benign or malignant disorders, are defined as abnormal cell proliferation in or around the brain [1][2]. Malignant tumours, like glioblastomas, sometimes develop quickly, are invasive, and are challenging to eradicate, whereas benign tumours, like meningiomas, normally do not spread to neighbouring tissues and develop slowly. Signs of elevated intracranial pressure, such as headaches, blurred vision, and emotional and cognitive disturbances, are caused by brain tumours that directly compress brain functioning [3][4]. The tumour may result in death or irreversible brain damage if it continues or becomes worse.

Furthermore, patients may suffer from a variety of health problems, ranging from minor memory loss to severe physical disability, contingent on the tumour's location and kind. For instance, medulloblastomas, which are more prevalent in children, usually arise from Gliomas, the most prevalent kind. Gliomas form in the cerebellum and impair balance and coordination, while the brain and spinal cord's glial cells give rise to malignant brain tumours in adulthood. Every kind of brain tumour has distinct biological characteristics. Traits, prognoses, and reactions to therapy.

To effectively treat brain tumours, various therapeutic approaches are usually needed. Chemotherapy and radiation are used to eradicate small remaining lesions or stop the tumour from growing further, while surgery attempts to remove as much of the tumour tissue as feasible. [5][6]. Therefore, a thorough understanding of the disease's many phases is essential for the successful prevention and brain therapy of tumours. However, diagnostic and treatment techniques also evolve with trends and technology, and they are only successful if detected early enough. Early

detection of any illness will lead to improved treatment [7]. Radiologic tests may ascertain the location and extent of a suspected brain tumour. The evaluation report is necessary for the next diagnostic and treatment planning purposes. Accurate and timely tumour detection is essential for the diagnosis.

In recent years, radiologists have examined brain tumours and used a range of imaging modalities, such as X-rays, to help with the accurate diagnosis and therapy selection. Magnetoencephalography (MEG), Ultrasound with Computed Tomography (CT), Electroencephalography (EEG), MRI, or magnetic resonance imaging. Primary brain tumours are difficult to detect early because they differ greatly in size, location, and other characteristics. Precisely defining absorption rates is essential for effective tumour imaging, as Non-invasive imaging techniques depend on the tissues' capacity for absorption to see tumours accurately [8]. Because MRIs, or magnetic resonance imaging, may provide information about the brain in healthy individuals and pathological conditions, it is notable for being the gold standard. When abnormalities occur, it helps identify the exact kind of tumour [9]. MRI is thus one of the finest clinical imaging modalities. [10]. However, MRI scan result analysis is hard for the average individual without careful observation and a high degree of skill. The drawn-out diagnosis procedure is further exacerbated by certain hospitals and healthcare facilities lacking the knowledge to satisfy these standards [11].

Rapid developments CNNs, or convolutional neural networks, are advanced technologies that have been developed in the fields of computer vision and machine learning. These cutting-edge models have effectively tackled challenging Computer-Aided Diagnosis (CAD) issues, including detection, segmentation, classification, and identification [12],[13],[14] and [15]. However, many current CAD methods for detecting brain tumours and detection that depend on CNNs are computationally intensive and inefficient across platforms. The lighter CNN classification model versions are inherently limited in accurately locating the tumour [16]. In contrast, segmentation models make tumour localisation possible, which use a mask to precisely pinpoint the damaged region, but at the penalty of increased computational expenses. Using common gadgets presents difficulties that result in ineffective operation and disappointing outcomes.

Researchers using either Deep learning (DL) or machine learning (ML) techniques [17],[18],[19], and [20] have published many traditional and contemporary brain tumour detection methods in the literature. The primary objective of the current automated and semi-automated disease evaluation procedure is to create a precise method for detecting diseases that will assist the physician with diagnosis and therapy planning.

Academics in the medical sciences have recently expressed significant interest in deep learning. This technology has significantly impacted clinical research, including illness detection, predictions, and identification. Deep methods for learning, like the Convolutional Neural Network (CNN) architecture, are used for segmentation and classification. These techniques provide an extensive understanding of radiology diagnosis, treatment, and interpretation [21]. This study attempts to resolve traditional issues while attaining superior outcomes with much-reduced computing effort and error rates. The method developed to automatically identify brain cancers is effective and reliable.

CNNs, or convolutional neural networks, such as the VGG-19 model are used to classify brain tumours. The proposed method utilizes VGG-19 transfer learning to increase the tumour detection's precision. When compared to conventional techniques, Deep learning algorithms have performed better in identifying brain tumours [22]. In particular, CNN-based Deep learning models have shown promising outcomes when classifying cancers from MRI scans.

This study presents an augmentation-based classification framework utilizing the VGG-19 transfer learning algorithm. VGG-19 serves as the foundation layer of the design, with activation, dropout, normalization, flattening, and dense layers coming next. Fine-tuning, parameter freezing, and transfer learning were used to maximize performance and minimize computing complexity.

OBJECTIVES

The following are the research's objectives:

- Implementing the VGG-19 convolutional neural network (CNN) model to improve MRI image classification accuracy for brain tumours.

- Developing an augmentation-based detection approach utilizing transfer learning with the VGG-19 algorithm to improve model robustness and generalization.
- Enhancing model efficiency by applying Bayesian optimization-based hyperparameter tuning to minimize computational complexity while maintaining high classification accuracy.
- To confirm the suggested model's efficacy, it will be compared with other deep learning models to demonstrate its efficiency over existing approaches.

METHODS

The VGG19 Architecture was created by the Oxford VGG19, the Visual Geometry Group's convolutional neural network. This design consists of 16 convolutional layers, as seen in Figure 1. A max-pooling layer comes after each group. These are followed by one softmax layer, five max-pool layers, and three completely linked layers. Unlike the other nets, this one allows you to practice with several settings, which may extend your exercise. Another benefit is that pre-trained weights from the image dataset are accessible. 224, 224, and 3 are the network input sizes. One convolution, a ReLU activation function, and a dimensionality reduction via the pooling layer are included in each convolution block. Lastly, the network uses the softmax activation function as its output to identify which of the 1000 categories the input falls into for the corresponding picture [23].

The suggested method uses to extract valuable information from MRI images, utilise VGG-19. Categorical image formats for rendering are revealed via visualisation. The extraction process takes into account important variables like circularity, pixel area, and perimeter to provide a trustworthy MRI that helps detect BT. 3x3 convolutional layers are put on top to enhance depth. VGG-19 is simple and effective. The processing layer is a top pool layer. method utilized in VGG-19 to reduce volume size. There are two 4096-neuron FC layers each.

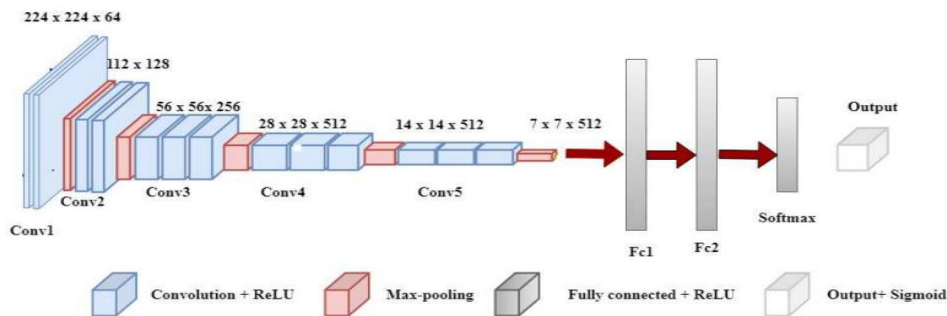


Figure 1 VGG-19 architecture [24]

This work offers a methodical way to classify brain tumours from MRI pictures using VGG-19. Data gathering, preprocessing, training-validation separation, model construction, and assessment are all included in the technique. The research uses fine-tuning and transfer learning strategies to improve the model's accuracy and efficiency. Pre-trained VGG-19 is used for classifying brain tumours, emphasising improving the model's robustness through augmentation-based learning strategies. The approach ensures high classification performance while maintaining scalability and generalization across MRI datasets. Algorithm 1 (Figure 2) illustrates the structure of our suggested brain tumour categorization model, integrating image processing and model prediction simultaneously.

A. Data Collection

This study's dataset was obtained from Kaggle, especially the "Brain MRI Scans for Brain Tumor Classification" collection. The collection includes MRI pictures of brain scans showing many kinds Numerous brain tumours, such as meningiomas, gliomas, pituitary, and non-tumour instances. The images in this dataset were pre-labelled with tumour categories for classification purposes. For training, the dataset was separated into three subsets for evaluation: test, validation, and training sets. These subsets were organized into distinct directories for effective data processing and analysis. The dataset can be accessed through the following Kaggle link: Brain MRI Scans for Brain Tumor Classification.

B. Dataset Description

MRI images spanning a variety of brain tumours and non-tumour conditions make up the dataset utilized in this investigation. Cases. These 2D and 3D images are carefully annotated to highlight the tumour regions, making it easier for machine-learning models to learn the relevant features. The tumours in the images are typically marked with bounding boxes in distinct colours, such as yellow or green, to indicate the affected areas. Additionally, the images are tagged with specific labels like "Tumor" or "Non-Tumor" to classify the nature of the scan. This information is essential for developing AI algorithms that can identify and categorise brain tumours, offering a useful tool for developing AI applications in medical imaging, especially for early brain tumour identification and detection. Figure 5 displays the pictures used to classify brain tumours.

C. Data Preprocessing

Data preparation is necessary to get the dataset ready for model training. Ensuring quality and consistency. The steps include:

- **Handling Missing Values:** Missing values are imputed using the feature's mean or median. The affected data points are removed if the missing values are too frequent.
- **Image Segmentation:**
- Image segmentation methods are used to differentiate and isolate the tumour regions from the healthy environment tissues. This step helps focus the model's attention on the relevant portions of the MRI images, making the classification task more efficient. Common segmentation techniques like thresholding or region-based segmentation are applied to detect and delineate tumour areas.
- **Normalization/Standardization:** Numerical features are scaled to standardize the data, using Z-score normalization or Min-Max scaling and aid in the convergence of the model.
- **Encoding Categorical Variables:** Categorical variables, such as tumour types, are converted into numerical values by label encoding or one-hot encoding.
- **Data Augmentation:** To address class imbalances, augmentation methods like flipping, magnification, and rotation increase the diversity of tumour pictures for better model training.

D. Training-Test Split

There are two subsets of the dataset:

- **Training Set (80%):** Used for training models, including parameter tuning and optimization.
- **Testing Set (20%):** Utilized to evaluate the model's performance on unidentified data, ensuring unbiased testing of its ability to generalize.

The split ensures that each class (tumour and non-tumour) is well-represented in both sets, maintaining balanced distributions.

E. Model building

The process of building the model begins with selecting the VGG-19 architecture, a widely known CNN suitable for image classification applications. To identify brain cancers in MRI pictures, it uses transfer learning to improve pre-trained weights from the ImageNet dataset. The process of data preprocessing involves the normalization of pixel values and the application of methods like zooming, rotation and flipping to add data to enhance the generalization capability of the model. Bayesian optimization is used to adjust the hyperparameters to prevent computational complexity while ensuring the model's optimal performance. It trains using the backpropagation with Adam optimizer and then tests on a confusion matrix, F1-score, recall, accuracy, and precision measures. The final stage of dropout regularization prevents overfitting and refines and optimizes the model to ensure a robust performance in unseen MRI datasets. Flowchart representation of the classification process is illustrated in Figure 3.

F. Model Evaluation

After concluding the training and testing stages, uniform evaluation metrics are essential for evaluating the model's functionality in object identification. Key performance metrics include Accuracy, Precision, Recall and F1-Score.

Algorithm 1 Brain Tumor Classification Algorithm

- 1: **Step 1: Data Collection**
- 2: Collect MRI images from Kaggle's "Brain MRI Scans for Brain Tumor Classification" dataset.
- 3: Split dataset into three subsets: Training, Validation, and Test (80% training, 20% testing).
- 4: Label images into categories: Tumor (Glioma, Meningioma, Pituitary) and Non-Tumor.
- 5: **Step 2: Data Preprocessing**
- 6: **Handle Missing Values:** Impute missing values using mean or median or remove them if frequent.
- 7: **Image Segmentation:** Apply thresholding or region-based segmentation to isolate tumor regions.
- 8: **Normalization/Standardization:** Apply Min-Max scaling or Z-score normalization to pixel values.
- 9: **Encoding:** Convert categorical tumor labels into numerical values using one-hot or label encoding.
- 10: **Data Augmentation:** Apply rotation, zooming, and flipping to augment the training data for better generalization.
- 11: **Step 3: Model Building**
- 12: Use pre-trained VGG-19 CNN with ImageNet weights for transfer learning.
- 13: Fine-tune the VGG-19 model for the brain tumor classification task.
- 14: Perform Bayesian Optimization to tune hyperparameters.
- 15: **Convolution Layer:** Apply convolution operation at each layer.
- 16: **Optimization:** Use Adam optimizer and backpropagation for training the model.
- 17: **Dropout Regularization:** Apply dropout regularization to prevent overfitting.
- 18: **Step 4: Model Evaluation**
- 19: Evaluate the model on test data using the following metrics:
- 20: **Accuracy:**

$$Accuracy = \frac{TP + TN}{S}$$
- 21: **Precision:**

$$Precision = \frac{TP}{TP + FP}$$
- 22: **Recall:**

$$Recall = \frac{TP}{TP + FN}$$
- 23: **F1-Score:**

$$F1 = \frac{2 \times (Precision \times Recall)}{Precision + Recall}$$
- 24: **Step 5: Model Refinement**
- 25: Fine-tune the model by adjusting hyperparameters and applying dropout regularization to improve performance.

Figure 2 Algorithm for Brain Tumor Classification

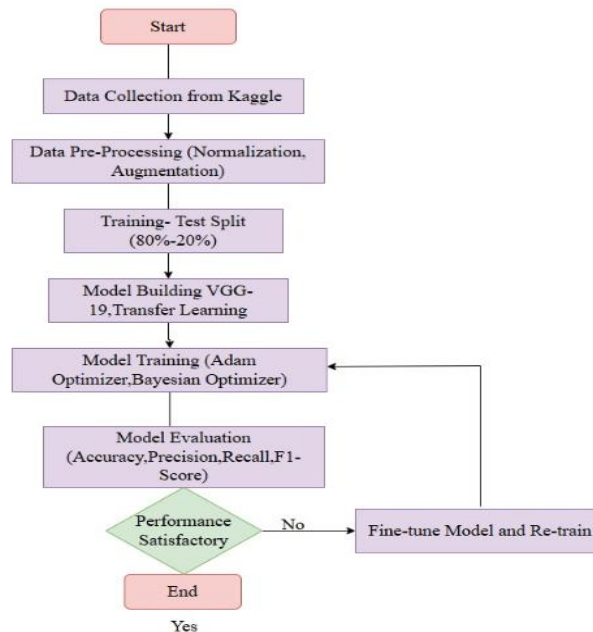


Figure 3 flowchart of proposed work

RESULTS

Table 1 Evaluation Metrics

Models	Accuracy	Precision	Recall	F1-Score
VGG-19	0.972	0.979	0.97	0.9792
ResNet-50 [25]	0.953	0.937	0.922	0.9468
GoogleNet [26]	0.964	0.9643	0.9654	0.9642

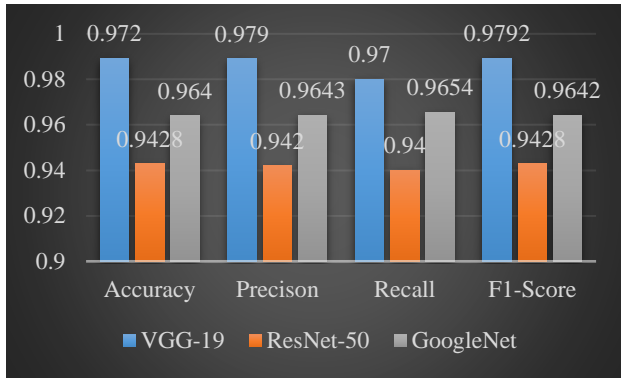


Figure 4 Comparison of Model Performance for Brain Tumor Classification Using Evaluation Metrics

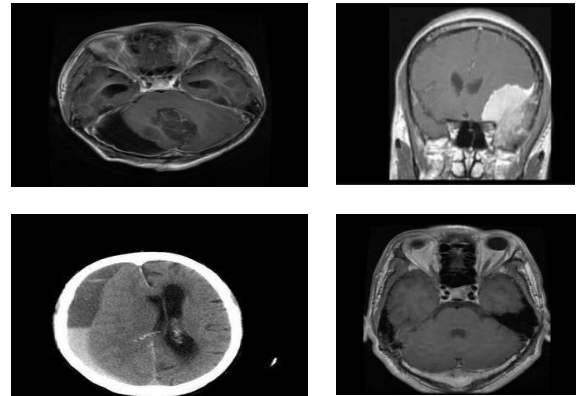


Figure 5 Brain MRI Scans for Brain Tumor Classification

The effectiveness of VGG-19, ResNet-50, and Google Net on a brain tumour classification task is presented through four critical metrics: F1-Score, Accuracy, Precision, and Recall (Ref. Table 1). A bar chart (Figure 4) showing the metrics would graphically present the models' relative strengths. VGG-19 achieved the highest performance. It reported an F1-score of 0.9792, precision of 0.972, a recall of 0.97, and an accuracy of 98.92%. The idea is that it not only creates highly accurate predictive results but also fairly balances precision with recall, providing the most authentic model for classifying the target. ResNet-50 takes a slight deviation from VGG-19 while achieving 95.3 per cent accuracy. On the other side, its respective F1 scoring, recall, and precision are 0.937, 0.922, and 0.9468, correspondingly. This means that though it is quite impressive, it also represents a minor diminishment compared to VGG-19's classification performance. GoogleNet, with an accuracy of 96.4%, outperforms ResNet-50 but is slightly below VGG-19. Its F1-score, recall (0.9654), and precision (0.9643) (0.9642) are well-balanced, showing a strong capacity to appropriately distinguish tumour and non-tumour cases.

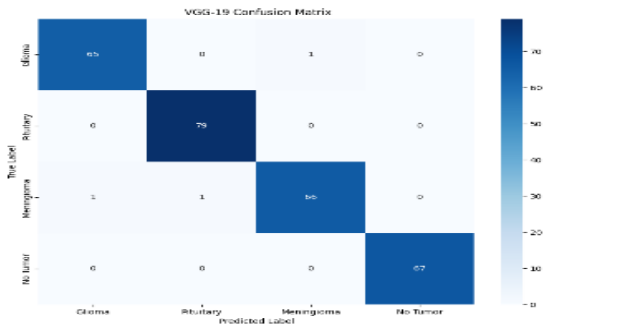


Figure 6 VGG-19 Confusion Matrix for Brain Tumor Classification

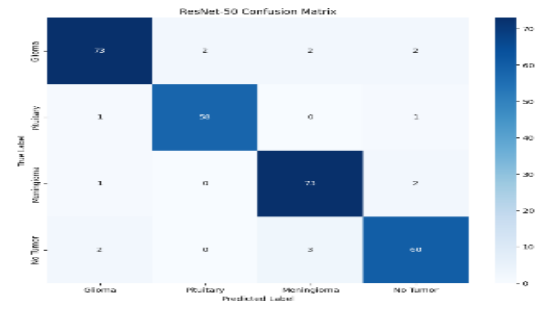


Figure 7 ResNet-50 Confusion Matrix for Brain Tumor Classification

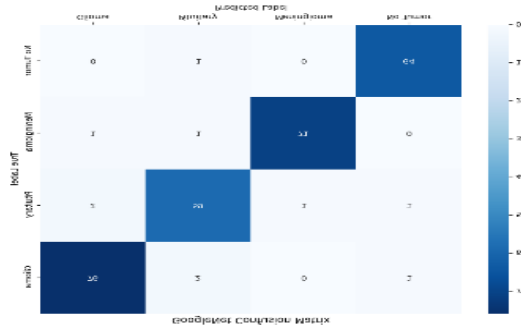


Figure 8 GoogleNet Confusion Matrix for Brain Tumor Classification

A bar chart of these values would clearly show that VGG-19 has the best accuracy and F1-score, while Google Net and ResNet-50 have followed. It would further depict that it's actually performing a little more efficiently in precision and recall than ResNet-50, which leaves GoogleNet as a competitive alternative. Overall, the bar chart will indicate visually that GoogleNet and then ResNet-50 best followed VGG-19.

The confusion matrices show the outcomes of the categorization process. Three deep neural network models tested—VGG-19, ResNet-50, and GoogleNet—including a classification output that can range over Meningioma, Pituitary, Glioma, and No Tumour are the four different classifications. Confusion matrices show the number of how well or badly the models have predicted classifications, with better performances shown for cases where elements in the main diagonal are of greater darkness in shade.

VGG-19 Confusion Matrix (Figure 6). This shows an excellent classification across all the tumours. The figure classifies Glioma into 69, Pituitary into 79, Meningioma into 66, and No Tumor into 67. A minor misclassification occurs in every category. That means that while robust, the model is still wrong at some classifications.

ResNet-50 Confusion Matrix (Figure 7) shows similar performances but higher accuracy in classifying Glioma (73 correct classifications) and Meningioma (73 correct cases). More significant errors appear with Pituitary (only 59 correct classifications) and No Tumor (60 correct classifications).

GoogleNet Confusion Matrix (Figure 8) has the best accuracy in classifying Glioma, with 76 correctly classified. It performs par to ResNet-50 in the detection of Meningioma, with 71 correct classifications, while Pituitary detection accuracy stands at 59. No Tumor classification attains 64, slightly better than ResNet-50 but lower than VGG-19. Overall, GoogleNet seems to be the most reliable model for Glioma detection, and ResNet-50 is almost balanced in all categories. VGG-19 performs very consistently but slightly worse on Meningioma accuracy.

The ROC curves represent the performance of different models for deep learning, such as ResNet-50, VGG-19, and Google Net, in classifying brain tumours. Each curve plots the sensitivity to the false positive rate or the genuine favourable rate. The bend towards the top-left corner of the classifier will be excellent in this plot.

The VGG-19 model's ROC curve, which has an AUC of 0.97, is shown in Figure 9. This is high. Score, which means that VGG-19 has an excellent ability to classify tumour and non-tumour cases since an AUC value close to 1 represents excellent grouping. The ResNet-50 model's ROC curve is shown in Figure 10, with an AUC score of 0.95. Although a bit smaller than the value obtained from VGG-19, this still represents a very high number in terms of classification capability. This rapid growth close to the y-axis also proves that there is an overall minimization of false positives without sacrificing the number of true positives. Figure 11 illustrates the ROC curve for the model GoogleNet and an AUC score of 0.961. This performance is better than that of ResNet-50 but marginally lower than VGG-19. It follows the pattern of the other two models, indicating a good capability to differentiate photos of tumours from those without.

All three models showed high classification performance with AUC values above 0.95. In this context, VGG-19 performed with the highest AUC at 0.97, followed by GoogleNet at 0.961 and ResNet-50 at 0.95. This clearly suggests because models for deep learning are very efficient for brain tumour categorization, and the best one in the present context is VGG-19.

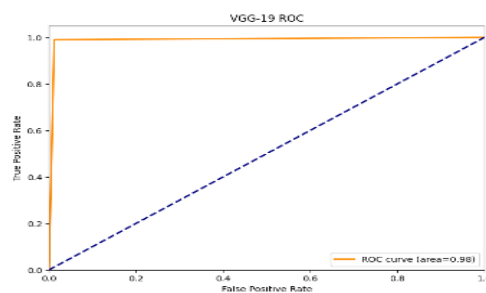


Figure 9 VGG-19 ROC Curve for Brain Tumor Classification

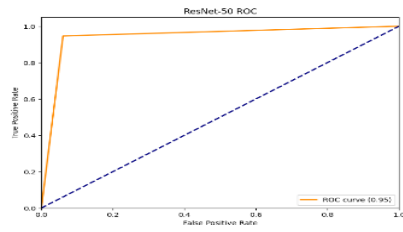


Figure 10 ResNet-50 ROC Curve for Brain Tumor Classification

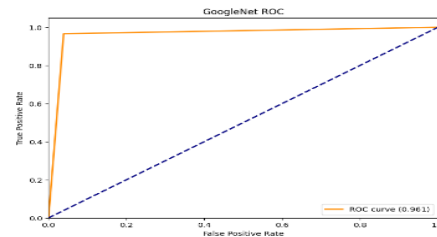


Figure 11 GoogleNet ROC Curve for Brain Tumor Classification

DISCUSSION

This research examined how well MRI data pictures were used by deep learning algorithms to classify brain tumours by comparing VGG-19, ResNet-50, and GoogleNet. The results of VGG-19 showed a performance of 97.2% accuracy, a recall of 0.97, precision of 0.972, and an F1-score of 0.9792. The one that balances precision and recall was also at its best, thus proving to be the most efficient classification model. The ResNet-50 and GoogleNet performed with high accuracy at 95.3% and 96.4%, respectively. GoogleNet outperformed ResNet-50 in precision and recall, but VGG-19 remained the most consistent and reliable. The confusion matrix analysis showed VGG-19's superior classification across all tumour types with minimal misclassifications. The ROC curve confirmed its robustness with the highest AUC score of 0.97. This study highlights the effectiveness of deep learning models, particularly VGG-19, in applications involving medical imaging. The research's future can improve accuracy by exploring transformer-based models or hybrid deep learning techniques. These models will be integrated into clinical decision support systems, improving early diagnosis and treatment planning. Increasing the dataset size with more MRI scans from diverse medical centres can enhance the generalization of models. The use of explainable AI would add trust and transparency to medical diagnoses. Overall, this study opens up the possibility of applying deep Learning to medical imaging, opening the door for AI-assisted diagnosis to enhance healthcare and patient outcomes efficiency.

REFERENCES

- [1] F. J. P. Montalbo, "A computer-aided diagnosis of brain tumours using a fine-tuned YOLO-based model with transfer learning," *KSII Trans. Internet Inf. Syst.*, vol. 14, no. 12, pp. 4816–4834, 2020.
- [2] M. M. Badža and M. Č. Barjaktarović, "Classification of brain tumours from MRI images using a convolutional neural network," *Appl. Sci.*, vol. 10, no. 6, p. 1999, 2020.
- [3] A. Dixit and P. Singh, "Brain tumour detection using fine-tuned YOLO model with transfer learning," in *Artificial Intelligence on Medical Data: Proceedings of International Symposium, ISCM 2021*, Springer, 2022, pp. 363–371.
- [4] E. Belykh, K. V Shaffer, C. Lin, V. A. Byvaltsev, M. C. Preul, and L. Chen, "Blood-brain barrier, blood-brain tumour barrier, and fluorescence-guided neurosurgical oncology: delivering optical labels to brain tumours," *Front. Oncol.*, vol. 10, p. 739, 2020.
- [5] M. A. Talukder et al., "An efficient deep learning model to categorize brain tumour using reconstruction and fine-tuning," *Expert Syst. Appl.*, vol. 230, p. 120534, 2023.
- [6] M. Woźniak, J. Siłka, and M. Wiczorek, "Deep neural network correlation learning mechanism for CT brain tumour detection," *Neural Comput. Appl.*, vol. 35, no. 20, pp. 14611–14626, 2023.
- [7] S. Giraddi and S. V Vaishnavi, "Detection of brain tumour using image classification," in *2017 International Conference on Current Trends in Computer, Electrical, Electronics and Communication (CTCEEC)*, IEEE, 2017, pp. 640–644.
- [8] Z. N. K. Swati et al., "Brain tumour classification for MR images using transfer learning and fine-tuning," *Comput. Med. Imaging Graph.*, vol. 75, pp. 34–46, 2019.
- [9] J. Watts, G. Box, A. Galvin, P. Brochie, N. Trost, and T. Sutherland, "Magnetic resonance imaging of meningiomas: a pictorial review," *Insights Imaging*, vol. 5, pp. 113–122, 2014.
- [10] A. R. Mathew and P. B. Anto, "Tumor detection and classification of MRI brain image using wavelet transform and SVM," in *2017 International conference on signal processing and communication (ICSPC)*, IEEE, 2017, pp. 75–78.
- [11] G. Litjens et al., "A survey on deep learning in medical image analysis," *Med. Image Anal.*, vol. 42, pp. 60–88,

- 2017.
- [12] A. S. Lundervold and A. Lundervold, "An overview of deep learning in medical imaging focusing on MRI," *Z. Med. Phys.*, vol. 29, no. 2, pp. 102–127, 2019.
 - [13] G. Alwakid, W. Gouda, M. Humayun, and N. Z. Jhanjhi, "Diagnosing melanomas in Dermoscopy images using deep learning," *Diagnostics*, vol. 13, no. 10, p. 1815, 2023.
 - [14] M. F. Almufareh, S. Tehsin, M. Humayun, and S. Kausar, "A transfer learning approach for clinical detection support of monkeypox skin lesions," *Diagnostics*, vol. 13, no. 8, p. 1503, 2023.
 - [15] A. Khan et al., "Optimizing connection weights of functional link neural network using APSO algorithm for medical data classification," *J. King Saud Univ. Inf. Sci.*, vol. 34, no. 6, pp. 2551–2561, 2022.
 - [16] Z. Q. Zhao, P. Zheng, S. T. Xu, and X. Wu, "Object Detection with Deep Learning: A Review," *IEEE Trans. Neural Networks Learn. Syst.*, vol. 30, no. 11, pp. 3212–3232, 2019, doi: 10.1109/TNNLS.2018.2876865.
 - [17] N. S. M. Raja, S. L. Fernandes, N. Dey, S. C. Satapathy, and V. Rajinikanth, "Contrast-enhanced medical MRI evaluation using Tsallis entropy and region growing segmentation," *J. Ambient Intell. Humans. Comput.*, pp. 1–12, 2024.
 - [18] P. Kanmani and P. Marikkannu, "MRI brain images classification: a multi-level threshold based region optimization technique," *J. Med. Syst.*, vol. 42, pp. 1–12, 2018.
 - [19] A. Gudigar, U. Raghavendra, T. R. San, E. J. Ciaccio, and U. R. Acharya, "Application of multiresolution analysis for automated detection of brain abnormality using MR images: A comparative study," *Futur. Gener. Comput. Syst.*, vol. 90, pp. 359–367, 2019.
 - [20] M. Buda, A. Saha, and M. A. Mazurowski, "Association of genomic subtypes of lower-grade gliomas with shape features automatically extracted by a deep learning algorithm," *Comput. Biol. Med.*, vol. 109, pp. 218–225, 2019.
 - [21] N. B. Bahadur, A. K. Ray, and H. P. Thethi, "Image analysis for MRI based brain tumour detection and feature extraction using biologically inspired BWT and SVM," *Int. J. Biomed. Imaging*, vol. 2017, no. 1, p. 9749108, 2017.
 - [22] S. A. A. Ismael, A. Mohammed, and H. Hefny, "An enhanced deep learning approach for brain cancer MRI images classification using residual networks," *Artif. Intell. Med.*, vol. 102, p. 101779, 2020.
 - [23] S. Mallick and S. P. Mishra, "An Automatic Detection of Brain Tumor using CNN & VGG19," 2023.
 - [24] A. R. Venmathi, S. David, E. Govinda, K. Ganapriya, R. Dhanapal, and A. Manikandan, "An automatic brain tumours detection and classification using a deep convolutional neural network with VGG-19," in *2023 2nd International Conference on Advancements in Electrical, Electronics, Communication, Computing and Automation (ICAECA)*, IEEE, 2023, pp. 1–5.
 - [25] M. B. Sahaai, G. R. Jothilakshmi, D. Ravikumar, R. Prasath, and S. Singh, "ResNet-50 based deep neural network using transfer learning for brain tumour classification," in *AIP Conference Proceedings*, AIP Publishing, 2022.
 - [26] A. Sekhar, S. Biswas, R. Hazra, A. K. Sunaniya, A. Mukherjee, and L. Yang, "Brain tumour classification using fine-tuned GoogLeNet features and machine learning algorithms: IoMT enabled CAD system," *IEEE J. Biomed. Heal. Informatics*, vol. 26, no. 3, pp. 983–991, 2021.